Chaotic solutions in the quadratic integrate-and-fire neuron with adaptation

Gang Zheng[1]*, Arnaud Tonnelier[2]

[1]*LJK, Université de Grenoble, 51 rue des Mathématiques, 38041 Grenoble, France*
Gang.Zheng@imag.fr
[2]*INRIA, LJK, Inovallée 655 Avenue de l'Europe Montbonnot, 38334 Saint Ismier, France*
Arnaud.Tonnelier@inrialpes.fr

Abstract

The quadratic integrate-and-fire (QIF) model with adaptation is commonly used as an elementary neuronal model that reproduces the main characteristics of real neurons. In this paper, we introduce a QIF neuron with a nonlinear adaptive current. This model reproduces the neuron-computational features of real neurons and is analytically tractable. It is shown that under a constant current input chaotic firing is possible. In contrast to previous study the neuron is not sinusoidally forced. We show that the spike-triggered adaptation is a key parameter to understand how chaos is generated.

Keyword: QIF, Chaos, Poincaré map, Lyapunov exponent

1 Introduction

Neurons transform incoming stimuli into train of all-or-one electric events known as spikes. Precise spike times are believed to play a fundamental role in the encoding of information by neural systems. In this view, the spike time reliability is a key to understand the basis of the neural code [Mainen and Sejnowski, 1995]. It has been shown that the responses of neurons to time varying stimuli have high reliability with a precision of 1 ms or less [Mainen and Sejnowski, 1995], [de Ruyter van Steveninck et al., 1997], [Berry et al., 1997]. On the other hand, constant stimuli elicits spike trains with high variability. It has been primarily suggested that such variability in discharge times is due to accumulating noise. However, it could be due as well to a chaotic behavior [Hayashi et al., 1982], [Chacron et al., 2004]. In fact, the responses of a neuron to given stimuli over

*Corresponding Author, Tel: 0033 4 76 51 45 61, Fax: 0033 4 76 63 12 63

repeated trials could be different because of intrinsic noise but also because of the chaotic behavior of the neuronal dynamics.

The reproducibility of spikes has been largely investigated in theoretical studies. Simplified phenomenological neuron models of integrate-and-fire type are commonly used to explore the dynamical properties of neurons and particularly the robustness of neuron response [Tiesinga, 2002], [Brette and Guigon, 2003]. Chaotic solutions have been investigated for the leaky integrate-and-fire neuron [Coombes, 1999], [Chacron et al., 2004]. A time-varying injected currents combined with a periodic modulation of parameters are the minimal requirements to obtain chaotic solutions.

The leaky integrate-and-fire neuron has some obvious limitations and an extension to quadratic integrate-and-fire (QIF) neurons allows to describe the nonlinear spike-generating currents of real neurons. In this paper we show that adaptive QIF neuron can exhibit chaotic solutions under constant input current. This result corroborates the non-reliability of spike times observed experimentally when a constant current is injected into a neuron [Mainen and Sejnowski, 1995], [de Ruyter van Steveninck et al., 1997].

The paper is organized as follows. In section 2 the model is presented. We derive in section 3 the expression of the Poincaré map associated with the firing of a spike and use the Marotto theorem in section 4 to show that the adaptive QIF can exhibit chaotic dynamics. Numerical simulations are made in section 5 to support our analysis and to highlight the dynamical behavior of the model.

2 The model

We consider an adaptive quadratic integrate-and-fire model given by the following differential equations:

$$\frac{dx}{dt} = x^2 + a - y \tag{1}$$

$$\frac{dy}{dt} = \frac{b-y}{\tau(x)} \tag{2}$$

and the spike rules:

$$x(t^+) = q, if \;\; x(t) = h \tag{3}$$

$$y(t^+) = cy(t) + p, if \;\; x(t) = h \tag{4}$$

where x is the membrane potential and y a phenomenological variable that represents adaptation. Parameters a, h and q are respectively the constant input current, the peak of a spike (see below) and the reset value. Parameters b, c and p describe the adaptive current and we assume $c \geq 0$. Note that y can be seen as a recovery variable. The function $\tau(x)$ models the voltage-dependence of the adaptive variable time-constant. For a fixed voltage value x, the variable y approaches the equilibrium b with a time constant $\tau(x)$. In the following we consider $\tau(x) = \tau/x$ where τ is a positive constant. This choice approximates

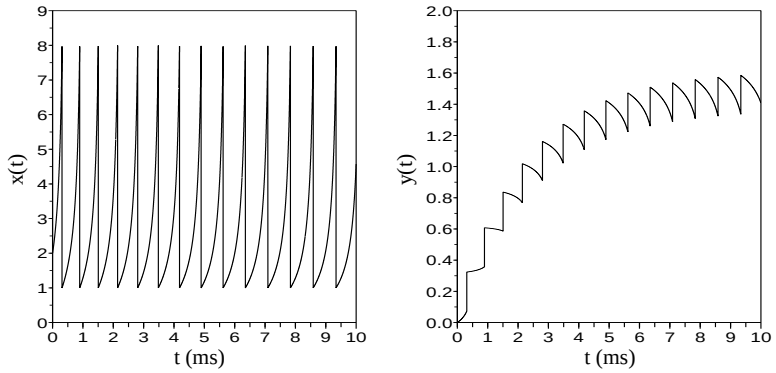

Figure 1: Illustrative plots of the time evolution for A: the membrane voltage $x(t)$, and for B: the adaptive variable $y(t)$ in the regular spiking regime. Parameters are $a = 2$, $\tau = 15$, $b = 1$, $q = 1$, $h = 8$, $c = 1$ and $p = 0.25$.

the voltage dependence of the time constant of the adaptive variable commonly used in detailed models: for large value of x the integration time of y is shorter. Therefore the time evolution of the adaptive current is given by

$$\frac{dy}{dt} = x(b - 2y)/\tau$$

where the factor 2 is used for convenience (see below) and can be removed (change of variables).

Because of the quadratic term in (1) the membrane potential can escape to infinity in finite time. We thus introduce h the cutoff of a spike that defines the firing of a spike. After a spike has been triggered the membrane potential restarts at a reset value q and the variable y is multiplied by a constant c and is increased by an amount p which accounts for spike-triggered adaptation. The differential equations (1)-(2) model the subthreshold dynamics and the spike initiation. When x attains the peak, the impulsive effect occurs according to (3)-(4). The time evolution is illustrated in Figure 1 for parameter values where the model exhibits regular spiking. Simulations (not shown) indicate that classical neuron-computational features of neurons [Izhikevich, 2004] including bistability, resonator and bursting (see later) can be reproduced by this model. For simplicity but without loss of generality, we consider $\tau = 1$ in the following analysis.

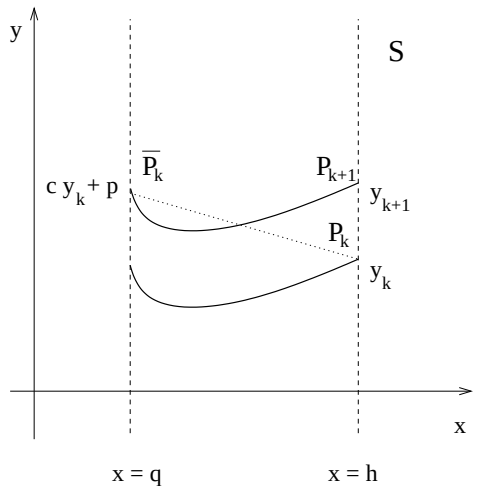

Figure 2: A piece of trajectory containing a jump (spike) in the phase plane (x, y). The vertical dashed lines are the reset line $x = q$ and the Poincaré section that corresponds to the threshold line $x = h$.

3 Poincaré map

Due to the non smooth nature of integrate-and-fire models, the standard theory of dynamical systems does not apply directly. This problem was overcome in previous studies using leaky integrate-and-fire model where a closed form for the map of successive firing times can be analytically derived. However, because of the nonlinearity of the subthreshold dynamics of the QIF it is no longer possible here to derive an analytical expression for this map. In order to analyze the behavior of system (1)- (4), we introduce the following Poincaré section: $\mathcal{S} = \{(x, y) \mid x = h\}$. It is easy to show that the differential system (1)-(2) is conservative. In fact, if we define the energy of the system as follows:

$$E(x, y) = \frac{1}{2}y^2 - y(a + x^2) + \frac{b}{2}x^2 \tag{5}$$

we have $dE/dt = 0$ along the trajectory of the system provided that no firing occurs. Let us now consider a trajectory that reaches the section $\mathcal{S}$ (the neuron fires) at point $P_k = (h, y_k)$, then according to the spike rules (3)-(4), the trajectory jumps to the point $\bar{P}_k = (q, cy_k + p)$ due to the impulsive effect (see Figure 2). After that the trajectory evolves according to (1)-(2), and it could reach again the section $\mathcal{S}$ at a point $P_{k+1} = (h, y_{k+1})$. Since $\bar{P}_k$ and P_{k+1} are both located on the trajectory of system (1)-(2) where no impulsive effect occurs, these two points satisfy relation (5). Consequently, we obtain:

$$\frac{1}{2}y_{k+1}^2 - \left(a + h^2\right) y_{k+1} + \frac{b}{2}h^2 = \frac{1}{2}\left(cy_k + p\right)^2 - \left(q^2 + a\right)\left(cy_k + p\right) + \frac{b}{2}q^2$$

and some straightforward calculations yield:

$$\left(y_{k+1} - a - h^2\right)^2 = \left(cy_k + p - a - q^2\right)^2 + \left(2a + h^2 + q^2 - b\right)\left(h^2 - q^2\right)$$

that defines an implicit map for the adaptive variable at the firing times. Assuming that $\forall k,\ y_k < a + h^2$ and setting $L = (2a + h^2 + q^2 - b)(h^2 - q^2)$, $H = a + h^2$, $Q = p - a - q^2$, then we can define the map f

$$y_{k+1} = f(y_k) = H - \sqrt{\left(cy_k + Q\right)^2 + L} \tag{6}$$

that gives the successive values of the adaptive variable at the firing times.

4 Chaotic behavior

In this section, with the help of Marotto's Theorem [Marotto, 1978], [Marotto, 2004] we prove that the adaptive QIF neuron (1)-(4) can exhibit chaotic behavior for specific values of parameters. The main idea of Marotto's theorem is to seek a snap-back repeller. Marotto showed that the presence of a snap-back repeller is a sufficient criterion for the existence of chaos. Let us first recall the basic Marotto's Theorem for one-dimensional system:

Theorem 1 *[Marotto, 1978] Let y_* be a fixed point of the map f. This fixed point is said to be a snap-back repeller if the following conditions are satisfied:*
(i) f is differentiable in a neighborhood $B_r(y_*)$ of the fixed point y_* with radius $r > 0$ and the eigenvalue of $Df(y)$ is strictly larger than one in absolute value for all $y \in B_r(y_*)$.
(ii) There exists a point $y_m \in B_r(y_*)$, with $y_m \neq y_*$, such that for some positive integer m, $f^m(y_m) = y_*$, and f^m is differentiable at y_m with $Df^m(y_m) \neq 0$.

A snap-back repeller arises when the fixed point is repelling while there is a trajectory starting in the repelling neighborhood of the fixed point that goes back to the fixed point, i.e. the repelling fixed point has an associated homoclinic orbit. Note that the existence of a snap-back repeller for one-dimensional system is closely related to the existence of a periodic point with period 3. In fact, it can be shown that the existence of a snap-back repeller of f is equivalent to the existence of a point of period 3 for the map f^n for some positive integer n [Li and Yorke, 1975].

Using Theorem 1 we will prove the following

Proposition 1 *For appropriate values of parameters the map f is chaotic in the sense of Marotto.*

In the remainder of this section we prove that the map f fulfills the conditions of Marotto theorem. In order to identify a snap-back repeller for the one dimensional map (6), we derive the eigenvalue of the system and show that, for

values of the state variable close to the fixed point, the corresponding eigenvalues lie outside the unit circle, whereas for values of the state variable that are sufficiently far from the fixed point, the eigenvalues are within the unit circle.

Let us firstly check whether condition (i) in Theorem 1 is satisfied. From (6) it is easy to show that the map has a fixed point $y_* = f(y_*)$ if the following inequality is fulfilled:

$$(cQ + H)^2 - \left(Q^2 - H^2 + L\right)\left(c^2 - 1\right) \geq 0 \tag{7}$$

which yields the following two fixed points:

$$y_* = \frac{\pm\sqrt{(cQ + H)^2 - (Q^2 - H^2 + L)(c^2 - 1)} - (cQ + H)}{c^2 - 1} \tag{8}$$

Moreover, according to (6) we have

$$Df(y) = -c\frac{cy + Q}{\sqrt{(cy + Q)^2 + L}}$$

where Df represents the derivative of f. The function Df is decreasing if

$$L \geq 0 \tag{9}$$

since $c > 0$. In addition, by defining $y_z = -\frac{Q}{c}$ it is easy to check that $f(y)$ is increasing if $y < y_z$ and is decreasing when $y > y_z$.

Let y_c be the solution of the equality: $Df(y_c) = -1$. Since $\lim_{y\to-\infty} Df = c$ and $\lim_{y\to+\infty} Df = -c$, a necessary and sufficient condition for the existence of y_c is

$$c > 1. \tag{10}$$

Moreover since $Df(y_c) < Df(y_z)$ and $Df(y)$ is decreasing when $y > y_z$, we have $y_c > y_z$.

Let us now consider a neighborhood of y_*, noted as $B_r(y_*)$, with

$$0 < r \leq min\{|y_* - y_c|, H - y_*\} \tag{11}$$

By construction, for all $y \in B_r(y_*)$, $Df(y)$ is always strictly larger than one in absolute values provided that $y_* > y_c > y_z$. Therefore, condition (i) of Theorem 1 is satisfied.

On the other hand, in order to fulfill condition (ii) of Theorem 1, we seek a point $y_m \neq y_*$ in the neighborhood $B_r(y_*)$, such that $y_{m-1} = f(y_m)$, ..., $y_1 = f(y_2) = f^{m-1}(y_m)$, and $y^* = f(y_1) = f^m(y_m)$, with some positive integer m, and $Df(y_k) \neq 0$, for $1 \leq k \leq m$.

Let us consider the following fixed point

$$y_* = \frac{\sqrt{(cQ + H)^2 - (Q^2 - H^2 + L)(c^2 - 1)} - (cQ + H)}{c^2 - 1} \tag{12}$$

and its neighborhood $B_r(y_*)$.

According to map (6), we have $y_* = f(y_1) = H - \sqrt{(cy_1 + Q)^2 + L}$ which yields two possible solutions: $y_{1,1} = \left(\sqrt{(y_* - H)^2 - L} - Q\right)/c$ and $y_{1,2} = \left(-\sqrt{(y_* - H)^2 - L} - Q\right)/c$. The first solution is identically equal to its corresponding fixed point, hence the possibility of existence of a snap-back repeller $y_m \in B_r(y_*)$ is relative to the second one, noted as y_1. Obviously we have $y_1 < y_*$.

Assume that the following conditions are satisfied:

$$\begin{cases} H > f(y_z) = y_A > y_* \\ f(y_A) = y_B < y_1 \end{cases} \tag{13}$$

Since $f(y_A) = y_B$ and $f(y_*) = y_*$, and $f(y)$ is a decreasing continuous function over $[y_*, y_A]$, therefore there always exists a point $y_2 \in]y_*, y_A]$, such that $y_1 = f(y_2)$. If such a y_2 is located in $B_r(y_*)$, we have $m = 2$. Otherwise, consider the interval $]y_1, y_z[$, since $y_* = f(y_1)$ and $y_A = f(y_z)$, and $f(y)$ is increasing over $[y_1, y_z]$, it is always possible to find a $y_3 \in [y_1, y_z]$ such that $y_2 = f(y_3)$. It should be noted that there exists another possible y_3 satisfying $y_2 = f(y_3)$, which is located over $[y_z, y_*]$. Notice that $y_* = f(y_*)$, $y_A = f(y_z)$, and $f(y)$ is decreasing over $[y_z, y_*]$, thus we can find the second $y_3 \in [y_z, y_*]$ such that $y_2 = f(y_3)$. Again if $y_3 \in B_r(y_*)$, then we found $m = 3$.

Otherwise, let us firstly consider $y_3 \in [y_1, y_z]$. With $f(y_2) = y_1$, $f(y_*) = y_*$, we get $y_4 \in [y_*, y_2]$ such that $f(y_4) = y_3$. If this y_4 is not yet located in $B_r(y_*)$, according to $f(y_3) = y_2$, $f(y_z) = y_A$, $f(y_*) = y_*$, since $f(y)$ is increasing over $[y_3, y_z]$ but decreasing over $[y_z, y_*]$, hence it always exists a $y_5 \in [y_z, y_*]$ such that $f(y_5) = y_4$. By induction, if the found points are not yet entered into $B_r(y_*)$, the above procedure generates the sequence: $y_B < y_1 < y_3 < y_z < y_5 < \cdots < y_* < \cdots < y_4 < y_2 < y_A < H$, which tends towards the equilibrium point y_*.

In order to prove the convergence of the above sequence to the fixed point y_*, let us analyze the right side of the sequence (i.e., even subscript), which in fact can be written as follows:

$$y_{2k} = f(f(y_{2k+2})) = H - \sqrt{\left(c\left(H - \sqrt{(cy_{2k+2} + Q)^2 + L}\right) + Q\right)^2 + L}$$

with $k \geq 1$. When $k \to \infty$, we have $y_{2k} = y_{2k+2}$, noted as y_{lim}. Obviously y_{lim} is one solution of equation: $y_{lim} = f^2(y_{lim})$, which in fact has two solutions under the constrain $y_* < y_{2k+2} < y_{2k} < H$. It is easy to check that equilibrium points of (8) are these two solutions. Since our analysis is focused only on the equilibrium point of (12), thus we have $y_{lim} = y_*$. It should be noticed that, for the left side of the sequence (odd subscript), we can obtain the same result through similar process, which implies the sequence converges towards the fixed point y_* via both two sides. Consequently, we can always find a point $y_m \in B_r(y_*)$, such that $f^m(y_m) = y_*$ with some positive integer m.

With the same procedure, it is easy to adapt the above proof for the second possible value of $y_3 \in [y_z, y_*]$.

Finally, since $Df(y_k) = -c\frac{cy_k+Q}{\sqrt{(cy_k+Q)^2+L}}$, hence if

$$y_k \neq -\frac{Q}{c} \tag{14}$$

we have $Df^m(y_k) \neq 0$. It is worth noting that if there exist some points such that $y_i = -\frac{Q}{c}$, then it corresponds to a periodic orbit of (6).

In summary, provided that the technical conditions: (7), (9)-(10), (13)-(14) are fulfilled, it is possible to determine a neighborhood $B_r(y_*)$ around the fixed point (12) with r defined in (11) such that conditions (i) and (ii) are satisfied. Therefore, Theorem 1 holds and this ends the proof of Proposition 1.

5 Numerical simulations

Besides the theoretical analysis, numerical simulations are made in order to show that system (1)-(4) can exhibit chaotic dynamics. In particular, we show that there exists parameter values for which the technical assumptions used in our proof are satisfied.

We consider the following QIF neuron with adaptation:

$$\begin{aligned} \frac{dx}{dt} &= x^2 + 6 - y \\ \frac{dy}{dt} &= x(2-2y) \end{aligned} \tag{15}$$

and the spike rules

$$\begin{aligned} x(t^+) &= 10, if \;\; x(t) = 20 \\ y(t^+) &= cy(t) - 0.2, if \;\; x(t) = 20 \end{aligned} \tag{16}$$

i.e. we choose the following set of parameter values: $a = 6$, $b = 2$, $\tau = 1$, $p = -0.2$, $q = 10$ and $h = 20$. We explore the influence of the parameter c on the asymptotic behavior of the model and we investigate the existence of adaptation-induced chaotic dynamics using different values for c.

For $c = 13.8$, we have $L = 153000$, $H = 406$ and $Q = -106.2$ that give the corresponding Poincaré map:

$$y_{k+1} = 406 - \sqrt{(13.8y_k - 106.2)^2 + 153000} \tag{17}$$

Numerically we check that inequality (7) is satisfied and straightforward calculations yield the following values for the variables introduced in the proof:

$$\begin{array}{lll} y_* \approx 11.4434, & y_c \approx 9.7957 & y_z \approx 7.6957, \\ y_1 \approx 3.9479, & y_A \approx 14.8479, & y_B \approx 2.5873 \end{array}$$

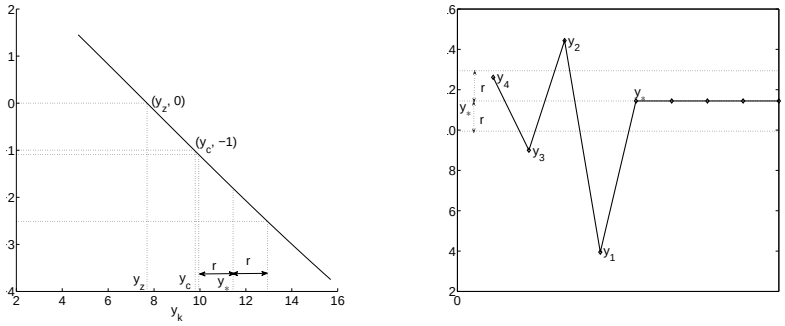

A *B*

Figure 3: Snap-back repeller of the QIF neuron with adaptation. The numerical investigations for the existence of a snap-back repeller are done in A and B, respectively. A: The derivative of the Poincaré map (17). The successive iterations y_k are represented in the neighborhood of the fixed point y_*. Numerically, we check that the absolute value of the derivative is always greater than 1 for all y_k. B: Location of the iterations with respect to the neighborhood of the fixed point y_*. We find $y_4 \in B_r(y_*)$ and $y_4 \neq y_*$ together with $f^4(y_4) = y_*$.

It is easy to check that conditions (9)-(10) and (13)-(14) are all satisfied. Moreover we choose $r = 1.5 < y_* - y_c$ that defines the neighborhood $B_r(y_*) =]9.9434, 12.9434[$ (see Figure 3A). Since we have $Df(9.9434) = -1.0909$ and $Df(12.9434) = -2.5123$, thus for all $y_k \in B_r(y_*)$, condition (i) of Theorem 1 is fulfilled.

It is easy to check that, for a $y_4 \approx 12.6150 \in B_r(y_*)$ and $y_4 \neq y_*$, we have $y_3 = f(y_4) \approx 9.0005$, $y_2 = f(y_3) \approx 14.4336$, $y_1 = f(y_2) \approx 3.9479$ and $y_* = f(y_1)$ (see Figure 3B). Moreover $Df^4(y_4) \approx -8.6461 \neq 0$, hence condition (ii) of Theorem 1 is satisfied. Consequently, the point y_* is a snap-back repeller and the map (6) exhibits chaotic behavior.

Besides the existence of chaos, the scenario leading to such dynamics as c varied is illustrated in Figure 4. The phase portrait of system (15)-(16) is shown together with the membrane potential as a function of time. When $c = 10$, the system tends towards an asymptotically stable periodic orbit (See Figure 4A,B). In Figure 4C,D, for $c = 13.9$ a period 3 solution occurs. A chaotic behavior can be generated by choosing $c = 13.8$ as shown in Figure 4E,F.

To gain deeper understanding of the chaotic dynamics, the bifurcation diagram obtained while varying parameter c is shown in Figure 5A, while Figure 5B shows the leading Lyapunov exponent of the system. The lines in the bifurcation diagram correspond to periodic spiking and the thick parts are associated with regimes where the adaptive variable takes either a countable but very large number of values or an uncountable value. It is not clear that in the bifurcation

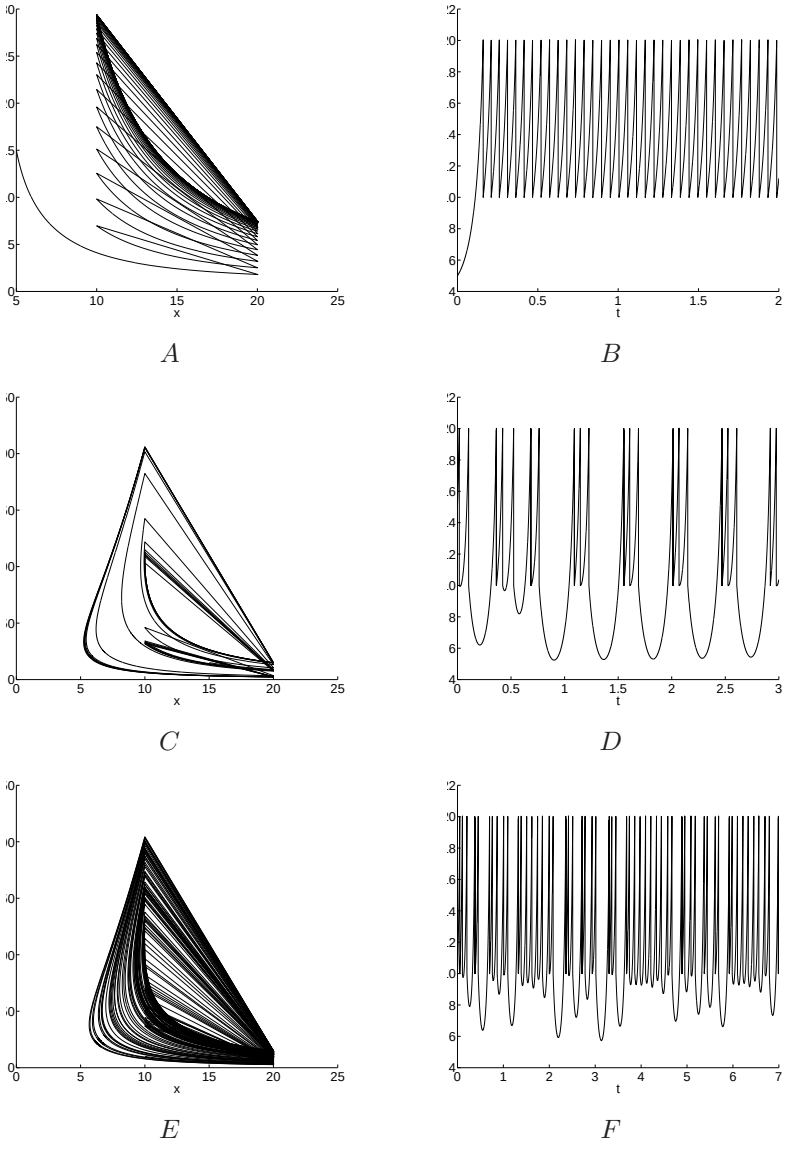

Figure 4: Transition to chaos through a cycle of period 3 in the QIF neuron with adaptation. The phase portraits are given in the left column and the x dynamics towards time are depicted in the right column. A, B: Asymptotically stable orbit for system with $c = 10$. Simulation was made with initial conditions: $x_0 = 5$, $y_0 = 15$. C, D: Period 3 orbit obtained for $c = 13.9$. Initial conditions are $x_0 = 15$, $y_0 = 15$. E, F: Chaotic orbit for system with $c = 13.8$ with initial conditions: $x_0 = 10$, $y_0 = 10$.

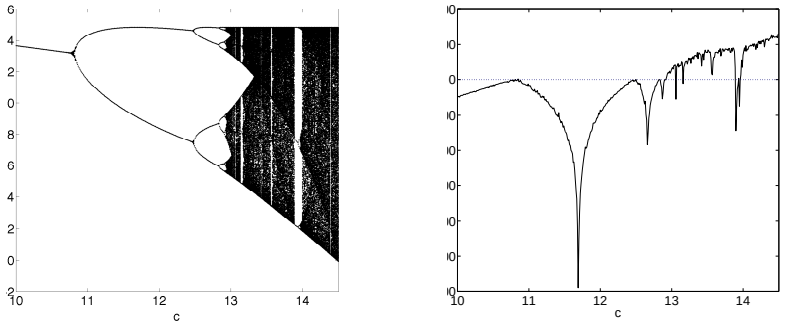

A *B*

Figure 5: A: Adaptive variable at the firing time, y_k, as a function of c illustrating the bifurcation diagram of our model. B: The corresponding variation of the lyapunov exponent with respect to parameter c. Simulation was made with initial conditions: $x_0 = 5$, $y_0 = 15$.

diagram the regimes where the adaptive variable takes a very large number of values are associated with periodic orbits with large period or chaotic regimes. One of the usual ways to test for chaos is to calculate system's largest lyapunov exponent. The Lyapunov exponent of a dynamical system is a quantity that characterizes the rate of separation of infinitesimally close trajectories. The general idea is to follow two nearby orbits and to calculate their average logarithmic rate of separation, and a positive Lyapunov exponent indicates chaos. According to expression (17), it is easy to calculate the largest lyapunov exponent and the result is shown Figure 5B. The range of positive exponent suggests chaotic regimes within these regions. Moreover the bifurcation diagram reveals that the system exhibits transition to chaos through period doubling bifurcation cascade.

6 Conclusion

Periodically forced integrate-and-fire neurons have been proposed to produce chaotic firing. It is expected that chaos in neuronal models can be generated through an applied constant current in agreement with the experimentally observed neural spike trains variability in this condition. This paper presents a simple nonlinear integrate-and-fire neuron which can exhibit a chaotic behavior under a constant current. The model is the quadratic integrate-and-fire neuron with a nonlinear adaptive current that takes into account the voltage dependence of the adaptive-variable time constant. The situation significantly differs from those in previous studies that report chaos in integrate-and-fire models for several reasons: (i) there is no periodic forcing (ii) threshold or resetting voltage

is not periodically modulated and (*iii*) the integrate-and-fire model is nonlinear. We proved mathematically the existence of chaotic solutions provided that parameters of the adaptive current are suitably chosen. Numerical simulations are given including the largest Lyapunov exponent and the bifurcation diagram.

A further development of this work is the study of entrainment in sinusoidally driven adaptive QIF neuron. It is expected that the model exhibits specific dynamics in response to periodic forcing that do not exist in LIF models. Further research is needed to clarified this point.

References

[Berry et al., 1997] Berry, M. J., Warland, D. K., and Meister, M. (1997). The structure and precision of retinal spike trains. *PNAS*, 94:5411–5416.

[Brette and Guigon, 2003] Brette, R. and Guigon, E. (2003). Reliability of spike timing is a general property of spiking model neurons. *Neural Comp.*, 15:279–308.

[Chacron et al., 2004] Chacron, M. J., Longtin, A., and Pakdaman, K. (2004). Chaotic firing in the sinusoidally forced leaky integrate-and-fire model with threshold fatigue. *Physica D*, 192:138–160.

[Coombes, 1999] Coombes, S. (1999). Liapounov exponents and mode-locked solutions for integrate-and-fire dynamical systems. *Phys. Lett. A*, 255(1-2):49–57.

[de Ruyter van Steveninck et al., 1997] de Ruyter van Steveninck, R. R., Lewen, G. D., Strong, S. P., Koberle, R., and Bialek, W. (1997). Reproducibility and variability in neural spike trains. *Science*, 275:1805–1808.

[Hayashi et al., 1982] Hayashi, H., Ishizuka, S., Ohta, M., and Hirakawa, K. (1982). Chaotic behavior in the onchidium giant neuron under sinusoidal forcing. *Phys. Lett. A*, 88:435–438.

[Izhikevich, 2004] Izhikevich, E. M. (2004). Which model to use for cortical spiking neurons? *IEEE Trans. Neural Networks*, 15:1063–1070.

[Li and Yorke, 1975] Li, T.-Y. and Yorke, J. A. (1975). Period three implies chaos. *Amer. Math. Monthly*, 82:985–992.

[Mainen and Sejnowski, 1995] Mainen, Z. F. and Sejnowski, T. J. (1995). Reliability of spike timing in neocortical neurons. *Science*, 268:1503–1506.

[Marotto, 1978] Marotto, F. R. (1978). Snap-back repellers imply chaos in r^n. *J. Math. Analysis and Appl.*, 63:199–223.

[Marotto, 2004] Marotto, F. R. (2004). On redefining a snap-back repeller. *Chaos, Solitons and Fractals*, 25:25–28.

[Tiesinga, 2002] Tiesinga, P. H. E. (2002). Precision and reliability of periodically and quasiperiodically driven integrate-and-fire neurons. *Phys. Rev. E*, 41913.